Duker, N. J., & Gallagher, P. E. (1988) *Photochem. Photobiol. 48*, 35-39.
Ehmann, U. K., Cook, K. H., & Friedberg, E. C. (1978) *Biophys. J. 22*, 249-264.
Grafstrom, R. H., Park, L., & Grossman, L. (1982) *J. Biol. Chem. 257*, 3465-3473.
Husain, I., Carrier, W. L., Regan, J. D., & Sancar, A. (1988a) *Photochem. Photobiol. 48*, 233-234.
Husain, I., Griffith, J., & Sancar, A. (1988b) *Proc. Natl. Acad. Sci. U.S.A. 85*, 2558-2562.
Kittler, L., & Löber, G. (1977) in *Photochemical and Photobiological Reviews* (Smith, K. C., Ed.) pp 39-131, Plenum Press, New York.
LaBelle, M., & Linn, S. (1982) *Photochem. Photobiol. 36*, 319-324.
Manley, J. L., Fire, A., Cano, A., Sharp, P. A., & Gefter, M. L. (1980) *Proc. Natl. Acad. Sci. U.S.A. 77*, 3855-3859.
Mellon, I., Spivak, G., & Hanawalt, P. C. (1987) *Cell 51*, 241-249.
Mitchell, D. L. (1988) *Photochem. Photobiol. 48*, 51-57.
Mitchell, D. L., Haipek, C. A., & Clarkson, J. M. (1985) *Mutat. Res. 143*, 109-112.
Myles, G. M., Van Houten, B., & Sancar, A. (1987) *Nucleic Acids Res. 15*, 1227-1244.
Park, S. D., & Cleaver, J. E. (1979) *Nucleic Acids Res. 6*, 1151-1159.
Protic-Sablijc, M., Tuteja, N., Munson, P. J., Hauser, J., Kraemer, K. H., & Dixon, K. (1986) *Mol. Cell. Biol. 6*, 3349-3356.
Rao, S. N., & Kollman, P. A. (1985) *Photochem. Photobiol. 42*, 465-475.
Regan, J. D., & Setlow, R. B. (1974) *Cancer Res. 34*, 3318-3325.
Sancar, A., & Sancar, G. B. (1984) *J. Mol. Biol. 172*, 223-227.
Sancar, A., Franklin, K. A., & Sancar, G. B. (1984) *Proc. Natl. Acad. Sci. U.S.A. 81*, 7397-7401.
Tang, M., Hrncir, J., Mitchell, D., Ross, J., & Clarkson, J. (1986) *Mutat. Res. 161*, 9-17.
Thompson, L. H., Mitchell, D. L., Regan, J. D., Bouffler, S. D., Stewart, S. A., Carrier, W. L., Nairn, R. S., & Johnson, R. T. (1989) *Mutagenesis 4*, 140-146.
Wallace, S. S. (1988) *Environ. Mol. Mutagen. 12*, 431-477.
Wood, R. D., & Robins, P. (1989) *Genome* (in press).
Wood, R. D., Lindahl, T., & Robins, P. (1988a) In *Mechanisms and Consequences of DNA Damage Processing* (Friedberg, E. C., & Hanawalt, P., Eds.) pp 57-61, Alan R. Liss, New York.
Wood, R. D., Robins, P., & Lindahl, T. (1988b) *Cell 53*, 97-106.
Zelle, B., & Lohman, P. H. M. (1979) *Mutat. Res. 62*, 363-368.

Sequence-Dependent Variations in the ^{31}P NMR Spectra and Backbone Torsional Angles of Wild-Type and Mutant *Lac* Operator Fragments†

Steven A. Schroeder, Vikram Roongta, Josepha M. Fu, Claude R. Jones, and David G. Gorenstein*
Department of Chemistry, Purdue University, West Lafayette, Indiana 47907
Received March 20, 1989; Revised Manuscript Received June 16, 1989

ABSTRACT: Assignment of the ^{31}P resonances of a series of six sequenced-related tetradecamer DNA duplexes, $d(TGTGAGCGCTCACA)_2$, $d(TATGAGCGCTCATA)_2$, $d(TCTGAGCGCTCAGA)_2$, $d(TGTGTGCGCACACA)_2$, $d(TGTGACGCGTCACA)_2$ and $d(CACAGTATACTGTG)_2$, related to the *lac* operator DNA sequence was determined either by site-specific ^{17}O labeling of the phosphoryl groups or by two-dimensional ^1H-^{31}P pure absorption phase constant time (PAC) heteronuclear correlation spectroscopy. $J(H3'-P)$ coupling constants for each of the phosphates of the tetradecamers were obtained from ^1H-^{31}P *J*-resolved selective proton flip 2D spectra. By use of a modified Karplus relationship the C4′-C3′-O3′-P torsional angles (ϵ) were obtained. Comparison of the ^{31}P chemical shifts and $J(H3'-P)$ coupling constants of these sequences has allowed greater insight into those various factors responsible for ^{31}P chemical shift variations in oligonucleotides and provided an important probe of the sequence-dependent structural variation of the deoxyribose phosphate backbone of DNA in solution. These sequence-specific variations in the conformation of the DNA sugar phosphate backbone of various *lac* operator DNA sequences can possibly explain the sequence-specific recognition of DNA by DNA binding proteins, as mediated through direct contacts between the phosphates and the protein.

Lac Operator. A number of studies have been carried out both in solution and in the solid state to gain a better understanding of binding interactions between regulatory proteins such as the *lac* repressor and DNA operator sequences. Most efforts directed toward defining the binding specificity between amino acid sequences and DNA sequences have centered on hydrogen bonding to the acceptor/donor groups on the Watson-Crick base pairs in the major groove [cf. Landschulz et al. (1988); see also the critical discussion in Matthews (1988)]. At present we do not understand this "second genetic code" of protein-DNA recognition. Perhaps one reason for the inability to dissect the basis for this specificity is the em-

†Supported by the NIH (GM36281 and AI27744), the Purdue University Biochemical Magnetic Resonance Laboratory, which is supported by the NIH (Grant RR01077 from the Biotechnology Resources Program of the Division of Research Resources), the NSF National Biological Facilities Center on Biomolecular NMR, Structure and Design at Purdue (Grants BBS 8614177 and 8714258 from the Division of Biological Instrumentation), and the National AIDS Research Center at Purdue (AI727713).

0006-2960/89/0428-8292$01.50/0 © 1989 American Chemical Society

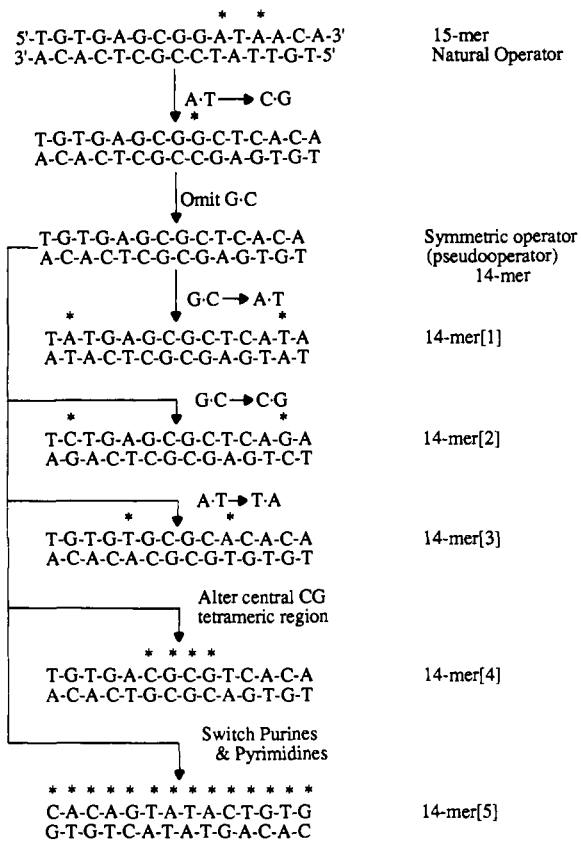

FIGURE 1: Natural operator, symmetric pseudooperator (14-mer), and mutant DNA sequences 14-mer[1], 14-mer[2], 14-mer[3], 14-mer[4], and 14-mer[5]. Asterisks indicate base-pair alterations relative to the 14-mer pseudooperator.

phasis on base-pair interactions alone. As described in this paper, the conformation and position of the phosphates appear to show sequence specificity, which may be an important component of protein-DNA recognition.

Although the results of a number of genetic studies suggest possible regions of contacts between the *lac* repressor and operator (Groeddel et al., 1978; Miller & Reznikoff, 1978; Takeda et al., 1983), the exact nature of the binding interaction on a molecular level is not known. The repressor protein recognizes and binds tightly to the operator DNA, a unique 21-base-pair sequence of the *Escherichia coli* chromosome. As described in this and a forthcoming paper (Schroeder et al., in preparation), we have assigned the ^{1}H and ^{31}P NMR spectra and in turn derived the 3D solution structure of the 14-base-pair *lac* "pseudooperator" segment d-(TGTGAGCGCTCACA)$_2$ and various mutants. This symmetrical base sequence is about two-thirds the length of the 21-base-pair wild-type sequence and is believed to contain most of the important contact sites (Simons et al., 1984). The 14-base-pair pseudooperator segment and various mutants are derived from the natural operator sequence as shown in Figure 1.

^{31}P NMR of Nucleic Acids. Nuclear magnetic resonance methods have developed as powerful probes of the structure and dynamics of DNA fragments in solution (Patel et al., 1987; Reid, 1987; Van De Ven & Hilbers, 1988; Gorenstein et al., 1989). While ^{1}H chemical shifts offer little information with regard to DNA structure, ^{31}P chemical shifts and ^{1}H–^{31}P coupling constants can provide valuable information on the phosphate ester backbone conformation (Gorenstein, 1984). Furthermore, ^{1}H–^{1}H 2D NOESY spectra give no direct information on the sugar phosphate conformation, and NOESY distance constrained structures are effectively disordered in this part of the structure (Van De Ven & Hilbers, 1988). However, a major limitation in the use of ^{31}P NMR in providing information on the backbone conformation has been the difficulty in assigning the signals. Conventional 2D heteronuclear correlation techniques were of limited value in resonance assignments for longer oligonucleotides (Pardi et al., 1983; Shah et al., 1984b), and regiospecific labeling of the phosphorus residues by selective ^{18}O and ^{17}O labeling proved quite useful (Petersheim et al., 1984; Schroeder et al., 1987; Shah et al., 1984b). Although this latter method provides unambiguous assignments of ^{31}P resonances, it suffers by being both time consuming and expensive with regard to the number of separate oligonucleotide syntheses required—for an oligonucleotide n nucleotides in length, $n - 1$ syntheses are required. Until recently, only oligonucleotide sequences six or less base pairs in length have been assigned by using the conventional HETCOR method (Cheng et al., 1982; Pardi et al., 1983; Shah et al., 1984b). Unfortunately, this NMR technique is limited by both spectral resolution and sensitivity, especially for longer oligonucleotides. However, newer reverse detection (Sklenář et al., 1986) and long-range, constant time HETCOR (Fu et al., 1988) methods have now been successfully applied to the ^{31}P assignment problem. Thus the assignment problems that initially held back the use of ^{31}P NMR have now been solved.

One of the main reasons for assigning ^{31}P resonances of oligonucleotides is to obtain information on the conformation of the phosphodiester bonds (Gorenstein, 1981, 1984, 1987; Gorenstein & Findlay, 1976). The internucleotidic linkage conformation is characterized by six torsional angles, which correspond to the six individual bonds that make up the linkage from one phosphate atom to the next along the DNA backbone. Theoretical studies have shown that the conformation of two of the six torsional angles (α, O3′–P–O5′–C5′, and ζ, C3′–O3′–P–O5′) appears to be most important in determining ^{31}P chemical shifts (Gorenstein, 1984, 1987; Gorenstein et al., 1988).

In duplex B-DNA, the gauche(−), gauche(−) (g^-,g^-; ζ, α) conformation[1] of the phosphate ester is energetically favored, and this conformation is associated with a more upfield ^{31}P resonance. In single-stranded DNA the trans, gauche(−) (t,g^-) conformation (as well as other staggered conformations about the P–O ester bonds) is also significantly populated due to the added flexibility of the random coil phosphodiester backbone, and the ^{31}P signal is observed more downfield in the ^{31}P NMR spectrum (Gorenstein, 1981; Gorenstein et al., 1976). The relative ^{31}P chemical shift difference between the two g^-,g^- and t,g^- conformational states is estimated to be 1.5 ppm.

In this paper, the ^{31}P chemical shifts and J(P–H3′) coupling constants of six different self-complementary 14-base-pair oligonucleotides (Figure 1) related to the operator sequence are reported [with the exception of the J(P–H3′) coupling constants for one of the 14-mers]. The mutant operator sequences 14-mer[1], 14-mer[2], and 14-mer[3] consist of two symmetry-related, base-pair changes from the "wild-type" pseudooperator 14-mer. Two additional 14-mer base-pair sequences, 14-mer[4] and 14-mer[5], have a greater number of base-pair changes. (14-mer[5] is not really related to the pseudooperator at all. In this sequence we switch all of the purine and pyrimidine nucleotides. This results in "identical" purine–pyrimidine base–pair steps and allows for a comparison

[1] Gauche(−) or −60° torsional angle; trans or 180° torsional angle. Crystal structures of duplex oligonucleotides show that these angles are only approximate and indeed the ζ angle is generally closer to −90° although we define this as "g^-".

of ^{31}P shifts that occur at common purine–pyrimidine steps having a different nucleotide sequence.)

Experimental Procedures

Materials. Nucleoside-derivatized porous glass support was either purchased from Applied Biosystems or prepared as described by Gait (1984). The amount of support loading was typically 25–30 mmol/g. The (dimethoxytrityl)deoxyribonucleoside phosphoramidites were purchased from either Beckman or Applied Biosystems. Capping solutions, acetic anhydride and 2,5-lutidine, were purchased from Applied Biosystems.

Sample Preparation. The self-complementary 14-mers were synthesized by a manual modification of the solid-phase phosphite triester method (using 10 μmol of the starting nucleoside derivatized support at a 28 mmol/g loading level for each separate synthesis) as previously described (Lai et al., 1984; Schroeder et al., 1987; Shah et al., 1984). The amounts of purified oligonucleotide obtained through one or more separate syntheses were 43.6 mg (871 OD units, 12.0 μmol) of 14-mer[1], 36.8 mg (737 OD units, 9.9 μmol) of 14-mer[2], 34.2 mg (685 OD units, 9.2 μmol) of 14-mer[3], 17.5 mg (351 OD units, 4.8 μmol) of 14-mer[4], and 24.6 mg (492 OD units, 6.8 μmol) of 14-mer[5]. The samples were desalted by dialysis in a cellulose, 1000 molecular weight cutoff dialysis tubing against double-distilled water. The samples were then treated with Chelex-100 cation-exchange resin. The purity of the 14-mers was verified by both reverse-phase (Altech C-18) and ion-exchange (Nucleogen column) HPLC as well as by ^{1}H and ^{31}P NMR spectroscopy.

^{31}P NMR samples were prepared by dissolving 4–20 mg (ca. 3 mM duplex) of the lyophilized DNA in 0.4 mL of buffer solution in D_2O containing 25 mM Hepes, 10 mM EDTA, 75 mM KCl, and 0.1 mM NaN_3, pH 8.0. Amounts of the 14-mers were determined spectrophotometrically by using the relationship of 20 absorbance units (optical density, OD units) per 1.0 mg of DNA per mL at 260 nm.

NMR Measurements. The ^{31}P 1D NMR spectra, the ^{31}P melting profiles, and the 2D ^{1}H–^{31}P correlation COLOC (PAC) and *J*-resolved spectra were run on a Varian XL-200A spectrometer at ambient temperature (ca. 20 °C) operating at 81.1 MHz. A sweep width of 172 Hz, acquisition time of 2.98 s, block size of 1K zero filled to 16K, and pulse width of 7 ms were used for the 1D spectra. Spectra were resolution enhanced by using a combination of positive exponential and Gaussian apodization functions. Typical values were 0.1–0.2 resolution enhancement values and 0.5–0.6 apodization function values, respectively. The values were adjusted in accordance to the signal to noise ratio in the ^{31}P NMR spectrum. The number of acquisitions for each spectrum was typically between 2000 and 3000. The ^{31}P resonances were referenced to an external sample of trimethyl phosphate (TMP) at 0.0 ppm, which is 3.53 ppm downfield of 85% phosphoric acid.

A ^{31}P–^{1}H *p*ure *a*bsorption phase *c*onstant time (PAC) version of the Kessler–Griesinger long-range heteronuclear correlation (COLOC) experiment (Kessler et al., 1984) was conducted on the 14-mers (Fu et al., 1988; Jones et al., 1988). The PAC spectrum provides chemical shift correlation between the H3′, H4′, and H5′ protons of the deoxyribose rings and the three or four bond coupled phosphorus. Coupling occurs between the phosphorus and the H3′ proton on the 5′ end and the H4′ and H5′ protons on the 3′ end of the dinucleotide fragment.

The Bax–Freeman selective 2D *J*-resolved long-range correlation experiment with a Dante sequence for the selective 180° pulse (Sklenář & Bax, 1987) was performed on the tetradecamers to correlate the ^{31}P chemical shift with the phosphorus–H3′ coupling constant. The *J*-coupled spectra were recorded at 18–50 °C. The data set was acquired with 256 points in the ^{31}P dimension and 32 t_1 increments and then zero filled to 512 × 128. Gaussian resolution enhancement was applied before Fourier transformation in both dimensions. *J* values were measured from peak center to peak center.

The observed three-bond coupling constant J(P–H3′) is used with a proton–phosphorus Karplus relationship to measure the H3′–C3′–O–P torsional angle θ from which we have calculated the C4′–C3′–O–P torsional angle ϵ ($=\theta + 120°$). The relationship $J = 15.3 \cos^2 \theta - 6.1 \cos \theta - 1.6$ was determined by Lankhorst et al. (1984) [see also Sklenář and Bax (1987)].

Results

Assignment of ^{31}P Signals of 14-mer Oligonucleotide Duplexes. Using the solid-phase phosphoramidite method, we have synthesized the six 14-base-pair deoxyoligonucleotide duplexes. The ^{31}P spectrum for each 14-mer is shown in Figure 2. [The ^{31}P spectra and assignments of parent 14-mer, 14-mer[1], 14-mer[2], and 14-mer[3] have previously been reported (Gorenstein et al., 1988) and are presented in the figure for comparison.] The ^{31}P signals of the tetradecamers were assigned by either a 2D pure adsorption phase constant time (PAC) heteronuclear correlation NMR (Fu et al., 1988) or $^{17}O/^{18}O$ labeling methodologies (Schroeder et al., 1987).

Although the ^{17}O labeling method is straightforward and provides unambiguous assignments of ^{31}P chemical shifts, it suffers by being rather expensive and time consuming. All mutant 14-mers were thus assigned by the 2D heteronuclear NMR methodology. As shown in Figure 3, assignment of the ^{31}P signal of the *i*th phosphate was achieved through connectivities with both the H3′(i) and H4′($i + 1$) or H5′($i + 1$)/H5″($i + 1$) deoxyribose protons—the proton signals had been previously assigned by the 2D ^{1}H–^{1}H spectra (Schroeder et al., in preparation). Although the H5′($i + 1$) and H5″($i + 1$) protons overlap with the 4′ protons, the intensities for the ^{31}P–H5′ and –H5″ PAC crosspeaks generally appear to be weaker than the H4′ crosspeaks.

Even though the "conventional" ^{31}P–^{1}H HETCOR experiment (with separate time periods for both frequency labeling and development of antiphase magnetization) was used to originally assign some of the H5′ and H5″ protons of the wild-type pseudooperator 14-mer (Schroeder et al., 1987), this method has been applied in ^{31}P assignment studies with success only for short DNA sequences, typically six or less nucleotides in length (Pardi et al., 1983; Shah et al., 1984b). For larger DNA sequences, the HETCOR experiment suffers from both poor sensitivity and resolution. This is mainly due to the interference of ^{1}H–^{1}H scalar couplings, which are more numerous and of the same magnitude as the ^{1}H–^{31}P couplings. As a consequence, ^{1}H–^{1}H coherence transfer competes with ^{1}H–^{31}P coherence transfer; the problem is magnified further since longer DNA fragments have short proton T_2's.

The conventional HETCOR spectrum required an acquisition period of 3 days (Schroeder et al., 1987), certainly providing significant experimental limitations. From a resolution standpoint, a single crosspeak width is about 0.5 ppm, which is approximately the entire range of the H3′ proton chemical shifts. In order to improve the heteronuclear experiment, modification of a ^{13}C–^{1}H HETCOR experiment was carried out to emphasize the small (2–6 Hz) ^{31}P–^{1}H scalar couplings (Fu et al., 1988). This COLOC (correlation spectroscopy via long-range coupling) experiment was originally designed to emphasize long-range ^{13}C–^{1}H couplings (Kessler

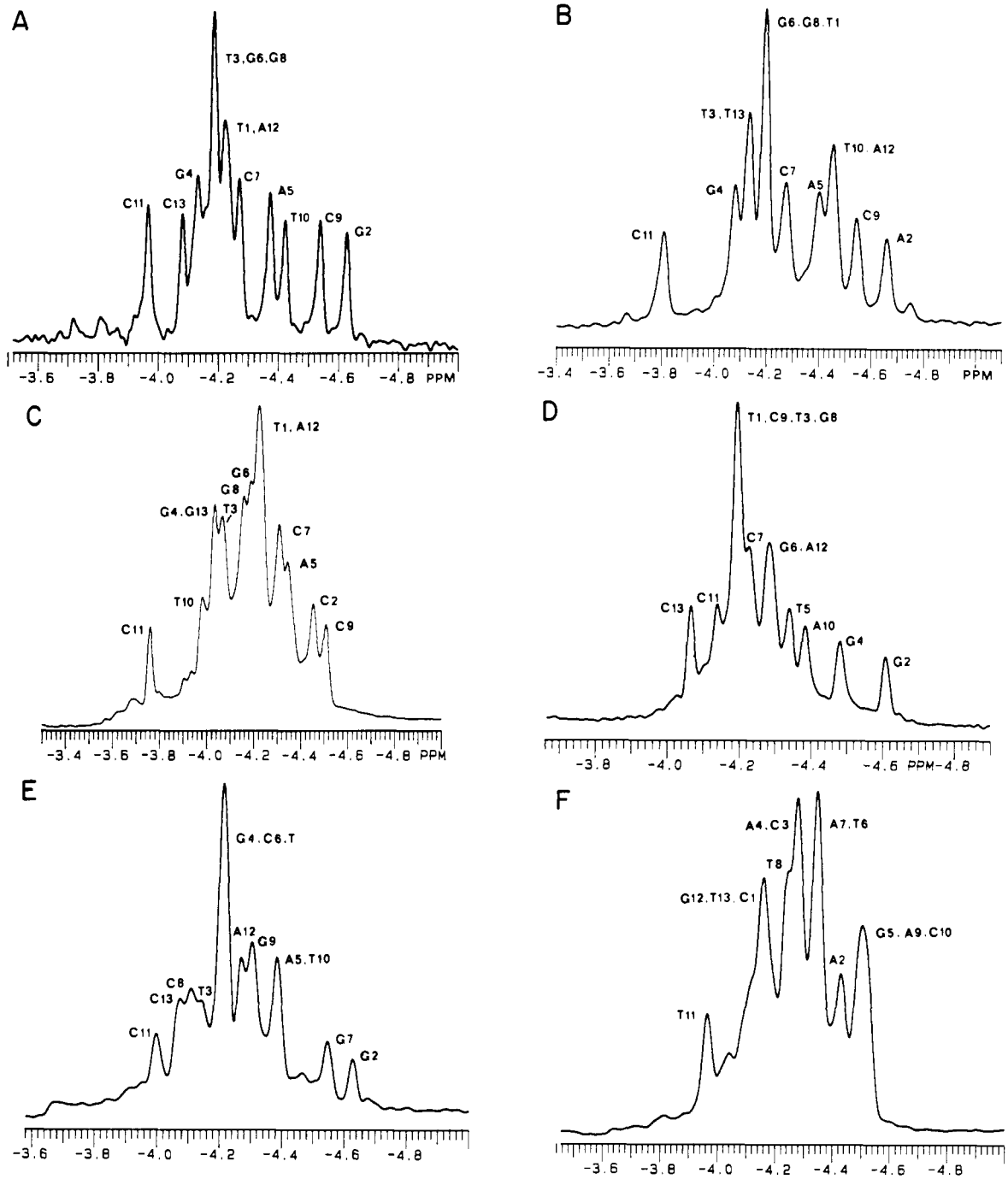

FIGURE 2: ^{31}P NMR spectra and phosphate assignments of 14-mer (A), 14-mer[1] (B), 14-mer[2] (C), 14-mer[3] (D), 14-mer[4] (E), and 14-mer[5] (F). Numbering corresponds to phosphate position from the 5′ end of the duplexes.

et al., 1984) that are of the same magnitude as the three-bond ^{31}P–^{1}H scalar couplings in oligonucleotides (Gorenstein, 1984).

In essence, the COLOC pulse sequence [and our pure absorption phase constant time (PAC) modification; Fu et al., 1988] incorporates both the evolution of antiphase magnetization and chemical shift labeling in a single "constant time" delay period, thereby improving the efficiency of coherence transfer and, as a consequence, increasing the sensitivity of the ^{31}P–^{1}H scalar coupling. Homonuclear decoupling during t_1, along with acquiring the spectrum in the phase-sensitive mode, can be used to improve spectral resolution (Kessler et al., 1984).

An example of the PAC spectrum and assignments for 14-mer[1] is shown in Figure 3A [the spectra and assignments of 14-mers[2]–[4] are shown in Figure 3B–D (see paragraph at end of paper regarding supplementary material), and the parent 14-mer spectrum may be found in Fu et al. (1988)]. The resonance assignments were made on the basis of the previously assigned H3′ assignments obtained from the 2D NOESY spectrum (Schroeder et al., in preparation). Note the increase in resolution when compared to the conventional ^{31}P–^{1}H HETCOR spectrum shown in Figure 3 of Schroeder et al. (1987). The sensitivity is also several times greater, since the PAC spectrum was acquired overnight. All 13 ^{31}P resonances of each of the 14-mer mutants were assigned in this fashion and are listed in Table I.

The following is a summary of the selected base-pair modifications and results for each of the mutant pseudooperator sequences.

14-mer[1] $d(TATGAGCGCTCATA)_2$. In this base-pair change (G-C → A-T, position 2) and complementary change at position 13 (C-G → T-A) the purine-pyrimidine sequence remains the same, and therefore the predicted helical distortions based upon the Calladine–Dickerson rules also remain

Table I: ^{31}P Chemical Shifts (ppm) and J(H3′–P) Coupling Constants (Hz) of 14-mers at 18 °C

14-mer	^{31}P shift	J(H3′–P)	14-mer[1]	^{31}P shift	J(H3′–P)	14-mer[2]	^{31}P shift
T	−4.23	3.6	T	−4.10	4.1	T	−4.28
G	−4.63	1.8	A	−4.64	nd	C	−4.51
T	−4.19	3.1	T	−4.18	4.8	T	−4.10
G	−4.14	5.6	G	−4.08	5.6	G	−4.08
A	−4.37	nd	A	−4.38	nd	A	−4.38
G	−4.19	3.1	G	−4.18	4.1	G	−4.20
C	−4.27	3.6	C	−4.25	4.7	C	−4.26
G	−4.19	3.1	G	−4.18	4.1	G	−4.19
C	−4.54	2.7	C	−4.53	3.5	C	−4.56
T	−4.42	2.7	T	−4.43	3.2	T	−4.02
C	−3.97	6.0	C	−3.82	nd	C	−3.76
A	−4.23	3.6	A	−4.42	3.9	A	−4.28
C	−4.09	5.3	T	−4.13	4.8	G	−4.02
A			A			A	

14-mer[3]	^{31}P shift	J(H3′–P)	14-mer[4]	^{31}P shift	J(H3′–P)	14-mer[5]	^{31}P shift	J(H3′–P)
T	−4.17	5.3	T	−4.19	6.1	C	−4.16	nd
G	−4.63	2.7	G	−4.63	2.3	A	−4.44	2.9
T	−4.14	3.6	T	−4.13	5.3	C	−4.25	3.5
G	−4.48	2.0	G	−4.20	5.8	A	−4.28	3.5
T	−4.32	5.2	A	−4.38	4.1	G	−4.52	2.6
G	−4.27	3.8	C	−4.17	6.1	T	−4.34	4.0
C	−4.22	5.6	G	−4.54	2.5	A	−4.04	nd
G	−4.18	5.6	C	−4.08	5.2	T	−4.23	4.0
C	−4.17	5.3	G	−4.29	5.0	A	−4.54	2.6
A	−4.37	3.1	T	−4.38	5.7	C	−4.50	2.6
C	−4.03	4.1	C	−3.97	5.4	T	−3.95	7.1
A	−4.22	3.8	A	−4.27	6.1	G	−4.37	4.4
C	−4.11	5.2	C	−4.04	6.1	T	−4.12	4.4
A			A			A		

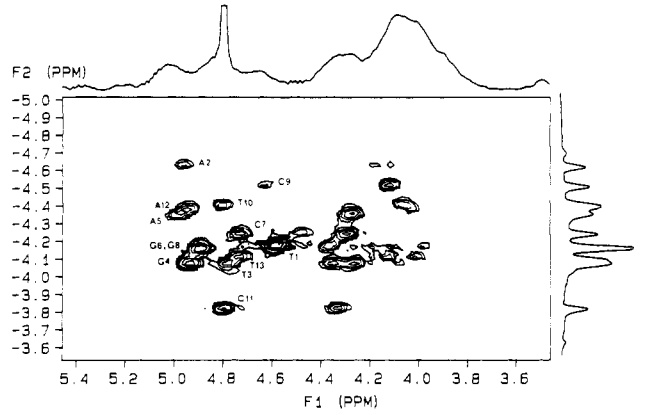

FIGURE 3: Two-dimensional ^{31}P–^{1}H PAC heteronuclear correlation NMR spectrum at 200 MHz (^{1}H) of duplex tetradecamers 14-mer[1] (A). The 1D decoupled ^{31}P NMR spectrum is shown along one axis, and the H3′, H4′, and H5′,5″ region of the proton spectrum is shown along the second axis.

the same (the rules are based upon generic purine–purine clash present in purine–pyrimidine or pyrimidine–purine base steps). This allows a comparison of the 5′-TGTG-3′/3′-ACAC-5′ terminal region which shows a large variation in ^{31}P shifts. The PAC spectrum of 14-mer[1] along with the identified P–H3′ scalar couplings is shown in Figure 3A. No ambiguities arose in assigning the resonances due to the resolved order of H3′ chemical shifts and the relatively resolved ^{31}P spectrum. The P–H4′ correlations match exactly with the assigned H4′ chemical shifts; however, no A(2)–P to T(3)–H4′ coupling is observed. Interestingly, T(13)–P shows a scalar coupling to the A(14)–H5′,H5″ protons, and scalar couplings of this type are not observed for any other residue in the sequence. Crosspeaks in the PAC spectra between the phosphate of residue 13 and the H5′,H5″ protons of residue 14 are observed in the other 14-mers and may be used to verify the ^{31}P assignment.

14-mer[2] d(TCTGAGCGCTCAGA)$_2$. A base-pair change (G-C → C-G) was carried out at position 2 (and again a complementary C-G → G-C change was made at position 13). The PAC spectrum of 14-mer[2] is shown in Figure 3B (see supplementary material). Besides the expected scalar coupling crosspeaks in the spectrum, two or three additional crosspeaks remain unidentified, for example, the two high-field crosspeaks flanking the C(9), C(2), and C(7) P–H3′ correlations. These crosspeaks were excluded in the assignments for three reasons. First, none correspond to a ^{31}P resonance in the ^{31}P spectrum; second, no H4′ correlations are associated with these crosspeaks; and third, no H3′ peaks corresponding to the ^{1}H correlations are seen in the 1D or 2D ^{1}H spectra. Because of the purity of the sample and the possibility of forming hairpin loops in palindromic sequences, we currently believe that these small crosspeaks arise from a minor hairpin loop conformation. Note that a hairpin loop would be expected to have longer transverse ^{31}P relaxation times which would selectively enhance the intensity of the PAC crosspeaks. From the order of H3′ assignments given in Schroeder et al. (in preparation), the purine ^{31}P assignments were straightforward. G(6)–H3′ and G(13)–H3′ protons were assigned identical chemical shifts in the NOESY spectrum; however, the two could still be distinguished, where G(6)–H3′ is slightly more upfield than G(13)–H3′. G(6)–P does not show any scalar coupling to a H4′ proton, but G(13) does show coupling to both A(14)–H5′,H5″ protons (4.10, 4.19 ppm) which were easily assigned in the NOESY spectrum. This type of coupling was also seen in the PAC spectrum of the pseudooperator and 14-mer[1]. The pyrimidine ^{31}P assignments were also straightforward from the assigned order of H3′ chemical shifts. Interestingly, the ^{31}P assignment associated with C(7) shows scalar couplings to the G(8)–H5′,H5″ protons, which suggests atypical coupling constants for these protons.

14-mer[3] d(TGTGTGCGCACACA)$_2$. The 14-mer sequence resulting from the base-pair changes at position 5 (A-T → T-A) and 10 (T-A → A-T) now represents an oligonucleotide sequence having an arrangement of completely alternating 5′-PyPu-3′ and 5′-PuPy-3′ base steps. The PAC spectrum is shown in Figure 3C (see supplementary material).

The ^{31}P resonance assignments were again straightforward with no ambiguities. G(8) and G(6) ^{31}P resonances were distinguished on the basis of their slightly different H3′ chemical shifts, where G(8)–H3′ is slightly more downfield than G(6)–H3′. C(11) and C(13) can be confirmed by their H4′ correlations to A(12) and A(14) residues, respectively. In addition, the ^{31}P resonance of C(13) shows a coupling to both the A(14)–H5′,H5″ protons, as observed in the PAC spectra of 14-mer[1] and 14-mer[2]. All of the ^{31}P–H4′ couplings correspond exactly to those assigned from the NOESY spectrum. Interestingly, A(12) does not show a coupling to the C(11)–H4′.

14-mer[4] d(TGTGACGCGTCATA)$_2$. The PAC spectrum of 14-mer[4] is shown in Figure 3D (see supplementary material). The six purine ^{31}P resonance assignments were identified easily from the more upfield purine H3′ chemical shifts. Two overlapping crosspeaks are obvious at around −4.28 ppm since the 1D ^{31}P spectrum shows only two peaks near this frequency. These ^{31}P resonances, G(7) and G(9), were distinguished via the corresponding H4′ correlations to C(8) (4.17 ppm) and T(10) (4.11 ppm). The pyrimidine assignments were made in a similar fashion. Two anomalous crosspeaks are evident, one occurring at −4.33 ppm and the other at −4.19 ppm. Again, neither one is associated with a ^{31}P resonance in the 1D spectrum. T(10) and C(11) have identical H3′ chemical shifts, but these two can be distinguished by their ^{31}P–H4′ correlations; in this case C(11) correlates with a purine H4′ while T(10) correlates with a pyrimidine H4′. A(5)– and G(2)–H4′ crosspeaks overlap once again, as in the previous PAC spectra, while as usual, C(13) shows a scalar coupling to the A(14)–H5′,H5″ protons.

14-mer[5] d(CACAGTATACTGTG)$_2$. The PAC spectrum is not shown (the spectrum is available upon request). All of the H3′ and H4′ scalar couplings can be identified except for one unidentified crosspeak at −4.10 ppm. Again, this crosspeak was eliminated from the assignment possibilities since it is a less intense ^{31}P resonance and is not associated with an H4′ correlation. All of the ^{31}P resonances were assigned in a straightforward manner by using the previously determined H3′ and H4′ chemical shifts. Although the position of the A(9) crosspeak is just slightly more downfield than A(2) (as in the NOESY spectrum), these two can be distinguished by their H4′ correlations to C(10) and C(3), respectively. Similarly, T(6) and T(7), having identical H3′ chemical shifts at 4.86 ppm, can be distinguished by using the H4′ correlations of A(7) and A(9). C(3) and C(10) were also distinguished in the same manner. The H4′ assignment of T(8) was not sufficiently resolved to yield a precise chemical shift; however, no chemical shift of this type is found more upfield than around −4.10 ppm. Therefore, the H4′ correlation associated with the A(7) ^{31}P resonance must be a T(8)–H5′, as is the A(2)–H5′ and G(14)–H5′ shown.

J-Correlated Spectra. The C4′–C3′–O–P torsional angle (ϵ) may be measured by the heteronuclear proton-flip experiment as optimized for P–H3′ coupling constants (Sklenář & Bax, 1987). These spectra were taken, without reverse detection, on the tetradecamer sequences, and one of the *J*-resolved ^{31}P–^{1}H spectra is shown in Figure 4 (other spectra not shown may be found in the supplementary material or will be provided upon request). The coupling constants were measured from the slice through the ^{31}P dimension for each of the separate ^{31}P resonances and are believed accurate to ±0.2 Hz (the slices show a well-resolved doublet). Table I lists the P–H3′ coupling constants measured at 18 °C. Combined with a proton–phosphorus Karplus relationship (see

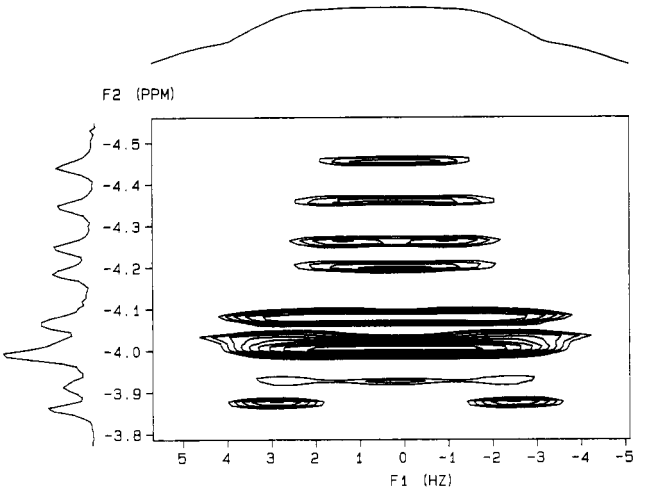

FIGURE 4: 2D ^{31}P–^{1}H *J*-resolved spectrum at 200 MHz (^{1}H) of duplex tetradecamer 14-mer at 18 °C. The 1D decoupled ^{31}P NMR spectrum is also shown along one axis, and the H3′ coupled doublets are shown along the second dimension.

Experimental Procedures), we can determine the H3′–C3′–O–P torsional angle θ from which we have calculated the C4′–C3′–O–P torsional angle ϵ. Up to four different torsional angles (0–360°) may be derived from the same coupling constant, and we assume that the ϵ torsional angle closest to the crystallographically observed value of −169° (Saenger, 1984) is the correct value. As shown by Dickerson (Dickerson, 1983; Dickerson & Drew, 1981), there is a strong correlation (R = −0.92) between torsional angles ζ and ϵ in the crystal structures of the dodecamer [ζ may be calculated from the relationship (Dickerson, 1983; Dickerson & Drew, 1981) ζ = −317 + 1.23ϵ]. Thus, assuming this correlation of ζ and ϵ exists for other duplex structures in solution as well, and from the measured coupling constants, we can calculate both C4′–C3′–O3′–P (ϵ) and C3′–O3′–P′–O5′ (ζ) torsional angles. A plot of the variation of ζ (and ϵ) vs ^{31}P chemical shifts for each of the tetradecamer sequences is shown in Figure 5. The correlation coefficient between ζ (or ϵ) and ^{31}P chemical shifts varies between 0.74 and 0.89 for the various 14-mers.

Discussion

^{31}P Chemical Shifts, Phosphodiester Conformation, and Calladine Rules. Studies carried out on model systems indicate that ^{31}P chemical shifts are dependent on the phosphate diester conformation (Gorenstein, 1981, 1983, 1984, 1987; Gorenstein & Findlay, 1976). ^{31}P chemical shifts of the wild-type and mutant pseudooperator sequences (and other duplex oligonucleotides) offer insight into those factors responsible for the variation of ^{31}P chemical shifts in oligonucleotides. One of the major contributing factors that determines ^{31}P chemical shifts is the P–O ester conformation (Gorenstein, 1984), defined by C3′–O3′–P–O5′ (ζ) and O3′–P–O5′–C5′ (α) torsional angles (Gorenstein, 1984). The more internal the phosphodiester linkage occurs within the oligomer sequence, the more constrained the torsion angles become, which can be attributed to an increase in double helical character of the oligonucleotide. More internal phosphates assume the lower energy, stereoelectronically favored g^-,g^- (ζ = −60°, α = −60°) conformation, whereas phosphodiester linkages located toward the two ends of the double helix tend to adopt mixtures between g^-,g^- and t (ζ; t = 180°),g^- (α), conformations, where an increased flexibility of the double helix is more likely to occur (Gorenstein, 1987). Studies carried out to investigate this relationship have determined that the g^-,g^- conformation is responsible for a more

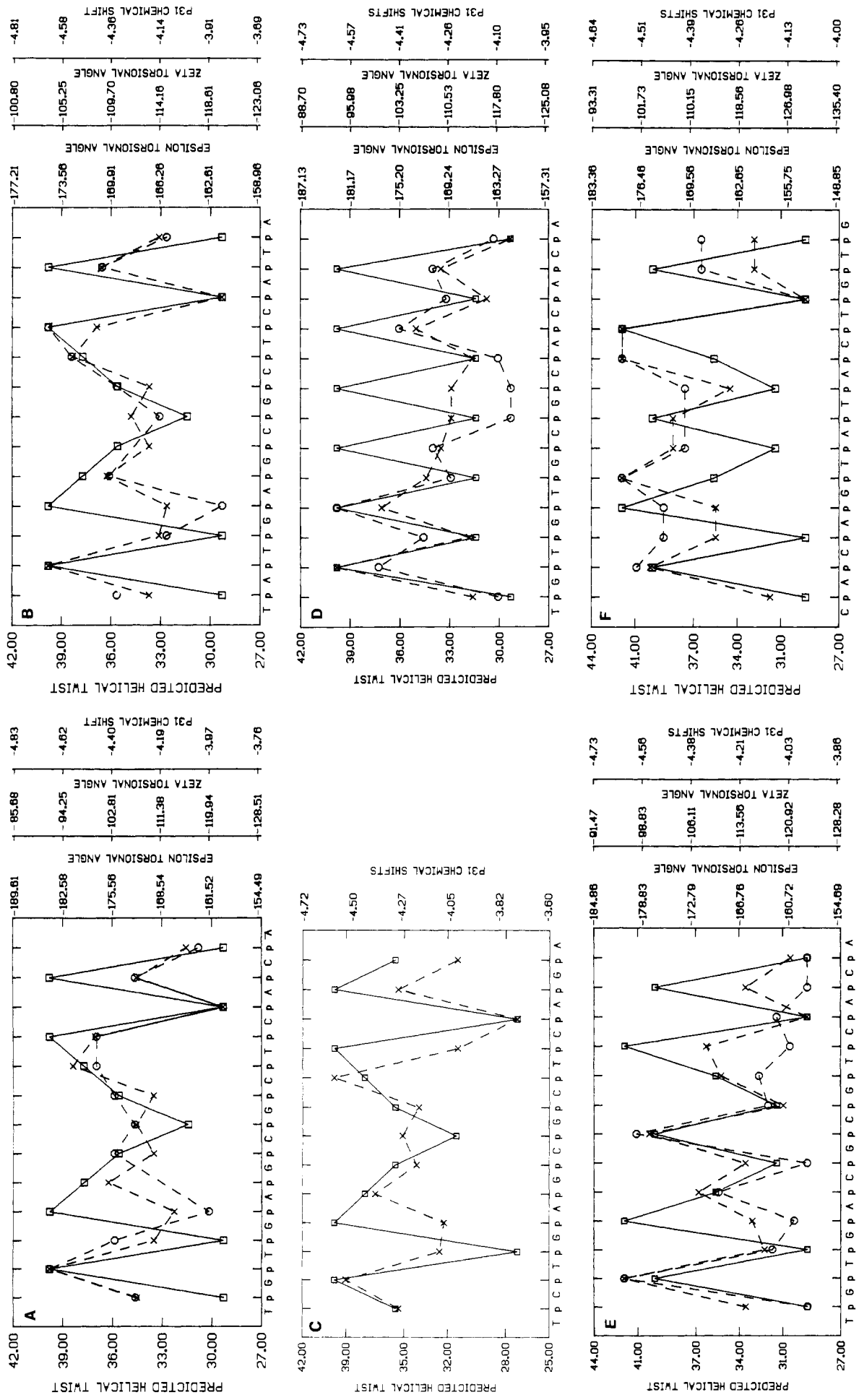

FIGURE 5: Comparison of ^{31}P chemical shifts (X) and experimentally measured $J(H3'-P)$ coupling constants as well as the P–O3′ ester torsional angle ζ and C–O3′ torsional angle ϵ (O) for the duplex tetradecamers 14-mer (A), 14-mer[1] (B), 14-mer[2] (C), 14-mer[3] (D), 14-mer[4] (E), and 14-mer[5] (F) vs position. ζ torsional angle from the Karplus relationship, and the correlation between ϵ and ζ ($\zeta = -317 - 1.23\epsilon$). Also shown is a plot of phosphate position vs calculated helix twist (□), t_g, derived from the calculated helix twist $\sum_1$ sum function and t_g ($=35.6 + 2.1\sum_1$). The t_g vs sequence plot has been scaled to reflect the ^{31}P chemical shift variations.

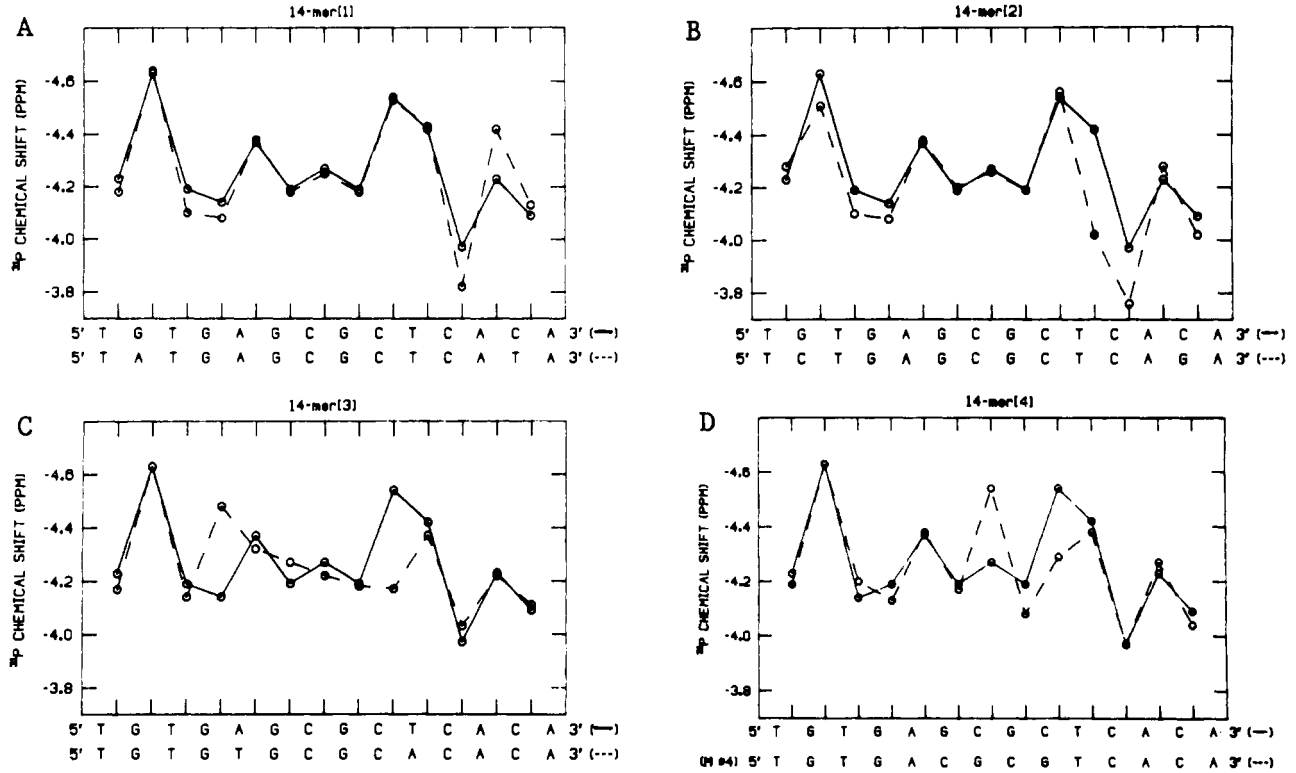

FIGURE 6: Comparison of the ^{31}P chemical shifts of pseudooperator 14-mers vs sequence. ^{31}P chemical shifts of 14-mer (dashed line in A–D), 14-mer[1] (solid line, A), 14-mer[2] (solid line B), 14-mer[3] (solid line, C), and 14-mer[4] (solid line, D).

upfield ^{31}P chemical shift, while a t,g^- conformation is associated with a lower field ^{31}P shift (Gorenstein, 1984). Of course, conformations in between these two states as well as different population mixes of the two state can exist and are associated with corresponding shifts in the ^{31}P resonance.

An additional factor other than position that could potentially affect the phosphodiester conformation would be local variations in parameters such as helix twist that occur along the duplex backbone. Sequence-specific, local conformational heterogeneity in the duplex structure has been noted in the crystal structures of duplex oligonucleotides (Calladine, 1982b; Dickerson, 1983; Dickerson & Drew, 1981). Sequence-specific variation in ^{31}P shifts has also been noted (Ott & Eckstein, 1985a,b; Schroeder, 1986; Gorenstein et al., 1988). The plots of helical twist, along with the variation in ^{31}P chemical shifts, are shown in Figure 5. The ^{31}P chemical shift variations of the three to four phosphates on each end of the 14-mers in the terminal region follow the predicted helical twist, while those in the middle region follow more closely the predicted roll angle adjustment [see Figure 9 in Gorenstein et al. (1988)]. Note that the helical twist predictions closely match the respective ^{31}P chemical shift variation at adjacent 5′-PuPy-3′ base steps relative to the 5′-PyPu-3′ position in each case.

Most significantly measured J(H3′–P) (and by inference ζ and ϵ torsional angles) also only follows the helix twist sum function pattern at the ends of the helix, just as is observed for the ^{31}P chemical shifts. This further substantiates the point we earlier made regarding the distinction between helix adjustment in response to steric clash at the ends versus the middles of the duplex (Gorenstein et al., 1988). Dickerson and Calladine have shown that sequence-specific helix distortions as measured by adjustments of the bases are well represented *throughout the entire helix* by the sum function relationships (except for the residue at each end of the helix).

Comparison of ^{31}P Resonance Assignments of 14-mer, 14-mer[1], 14-mer[2], and 14-mer[3]. Comparison of the ^{31}P chemical shifts of each mutant to that of the pseudooperator versus sequence is shown in Figure 6. The solid line in the plots is that of the pseudooperator, while the dashed lines represent the variations of the mutant sequences. Remarkably, the ^{31}P spectra and shift variation (Figure 6A) of mutant 14-mer[1] and the 14-mer are very similar despite the G → A and C → T changes at positions 2 and 13, respectively. As would be predicted from the sequence-specific effects, the variation from one base step to the next of 14-mer[1] remains the same, with some small variation observed at steps surrounding the base-pair alteration. Base steps that are two positions removed have ^{31}P shifts essentially identical with that of the pseudooperator. Surprisingly, larger differences occur at the 3′ end, while only subtle differences occur at the 5′ end, in contrast to the Calladine rules which predict equal effects at both ends. Both phosphate positions 11 and 12 are shifted in an "opposite" manner in 14-mer[1] by approximately the same amount. Note that the base-pair changes in 14-mer[1] relative to the 14-mer conserve the pattern of pyrimidine and purine base pairs, thus supporting our hypothesis that either purine G or A will produce comparable local helical adjustments in the phosphate ester backbone (similarly for the pyrimidines).

The ^{31}P chemical shift pattern of 14-mer[2] is also quite similar to that of the pseudooperator; however, the magnitude of the ^{31}P chemical shift perturbations is significantly greater than in 14-mer[1] (Figure 6B). 14-mer[2] mutation is again at positions 2 (G → C) and 13 (C → G). As in the 14-mer[1] mutation sequence, greater perturbations (relative to the wild-type pseudooperator) in the ^{31}P shifts are observed at the 3′ end of the sequence. These modifications cause the alternating purine–pyrimidine sequence at the terminal ends to be different and as a result change the alternating clash order from minor groove–major groove–minor groove to a single minor groove clash step at phosphate position 3 (now an isolated 5′-PyPu-3′ step without adjacent 5′-PuPy-3′ steps). Since a low-field ^{31}P chemical shift has been detected at every minor groove clash in the pseudooperator and 14-mer[1], it is not

surprising to see a similar downfield shift at position 3 in 14-mer[2]. Note that positions 1 and 13 are now homopolymer steps rather than a 5′-PyPu-3′ step as the result of the mutation at positions 2 and 12. It is thus surprising that the ^{31}P chemical shifts of phosphates 1 and 13 of 14-mer[2] are quite similar to those of the parent 14-mer (note that the chemical shifts at these positions for mutant 14-mer[1] are also quite similar). Additionally, the chemical shift of phosphate position 2, now being a homopolymer step, is unexpected. Apparently, the conformation arising from the lone TpG step at position 3 affects the adjacent CpT in the same fashion as the GpT step in the pseudooperator or 14-mer[1]. Of course, this is consistent with the interpretation that 5′-PyPu-3′ steps account more for helical distortions, as well as the observation that 5′-PuPy-3′ steps are equivalent to homopolymer steps. The slight difference in shift between the two positions probably is a result of sequence differences between 5′-GpT-3′/3′-ApC-5′ and 5′-CpT-3′/3′-ApG-5′ base steps.

The ^{31}P chemical shift patterns at positions 5–9 in the 14-mer, 14-mer[1], and 14-mer[2] are all the same (Figure 6A,B), as expected since these are equivalent positions in these three 14-mers. Interestingly, the perturbations in the ^{31}P chemical shifts between the 14-mer[2] and the parent 14-mer extend to phosphates at positions 4 and 10. As in the 14-mer[1], perturbations in ^{31}P shifts in the 14-mer[2] are more accentuated at the 3′ end. Note particularly the large 0.40 ppm downfield shift of phosphate 10 in 14-mer[2] relative to the same phosphate in the wild-type 14-mer. These steps are two positions away from the base–pair changes, indicating that backbone distortions are affected further away from the clash sites. The Calladine–Dickerson rules predict substantial changes at the clash site and smaller effects at the nearest-neighbor site on either side of the base step. Our ^{31}P results thus suggest that sequence effects can extend to structural perturbations in the backbone conformation further than the local helical parameters originally predicted by the Calladine–Dickerson rules.

Duplex 14-mer[3] represents mutations at positions 5 (A → T) and 9 (T → A). These modifications produce a 14-mer with completely alternating purine–pyrimidine sequence. In addition, phosphate positions that are now identical in both base sequence and purine–pyrimidine steps are as follows: 1, 3, and 5 (TpG); 9, 11, and 13 (CpA); 2 and 4 (GpT); and 10 and 12 (ApC). Note that the ^{31}P chemical shifts of phosphates 1–5 and 9–13 also completely alternate (first downfield, then upfield, downfield, etc.) in keeping with the alternating nature of the sequence (Figure 6C). However, in the central region (positions 5–9) there is no alternation of the ^{31}P chemical shifts. Phosphates at positions 5–8 have ^{31}P shifts very similar to those of the pseudooperator, and the loss of an alternating pattern represents quite small changes in ^{31}P chemical shifts in this central region (<0.1 ppm).

Not surprisingly, the ^{31}P shift variations at the two ends of 14-mer[3] (mutations occurring at positions 5 and 10) are identical with that in the pseudooperator. Phosphate positions 4 and 9 directly adjacent (both in the 5′ direction) to the mutations are most affected by the base-pair changes, while the central region is also only slightly affected. the 0.3–0.4 ppm perturbations produced in the ^{31}P chemical shifts of both phosphates 4 and 9 agree exactly with the predicted variations expected for the alternating purine–pyrimidine base steps. Phosphate 4 is shifted 0.34 ppm upfield relative to the parent 14-mer while phosphate 9 is shifted 0.37 ppm downfield.

Note also in all of these sequences that the actual ^{31}P shift is dependent on the position in the sequence. Identical base steps at more internal positions are associated with smaller changes in ^{31}P shift variation from one base step to the next. Undoubtedly, this is due to differences in helix flexibility between base steps located at the two ends and central regions. Thus the ^{31}P shifts of identical base steps also depend on position within the sequence.

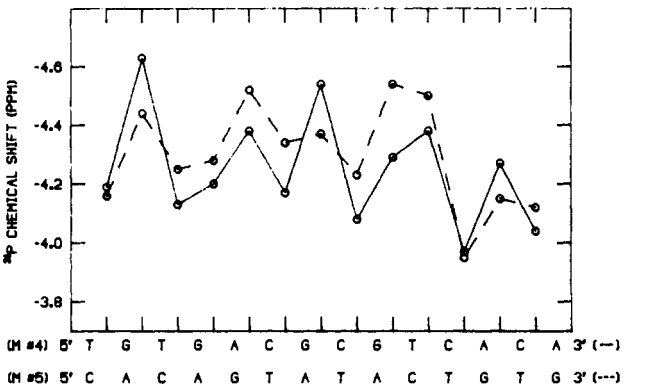

FIGURE 7: Comparison of the ^{31}P chemical shifts of pseudooperator 14-mer mutants [4] and [5] vs sequence. ^{31}P chemical shifts of 14-mer[4] (solid line) and 14-mer[5] (dashed line).

The ^{31}P chemical shift comparison of 14-mer, 14-mer[4], and 14-mer[5] is shown in Figures 6D and 7. 14-mer[4] represents multiple mutations at positions 6–9 involving G/C replacements, and not surprisingly, the only major ^{31}P chemical shift differences between the parent 14-mer and 14-mer[4] are found in the central region. At the two ends of 14-mer[4], nearly identical ^{31}P shifts to the parent 14-mer are observed, the only difference being at positions 3 and 4 where the ^{31}P shifts are just slightly different. Note that the ^{31}P shifts at positions on the 3′ side of the central region are more perturbed by the base-pair changes, consistent with that observed for the other 14-mer sequences studied. Excluding positions 3 and 4, the only step that the variation is different from the pseudooperator is at positions 9 and 10. This is analogous to 14-mer[2], where creation of a 5′-PyPu-3′ step (at position 8) affects the adjacent homopolymer base step in the same manner.

Even though the variation is identical for the central region where the changes occurred, the variation of 14-mer[4] is exactly "opposite" if one considers how the alternating purine–pyrimidine base steps were changed. That is, at the 5′-GpCpGpC-3′ steps in the 14-mer pseudooperator, the ^{31}P shift is downfield–upfield–downfield, respectively. In 14-mer[4], the variation for the 5′-CpGpCpG-3′ steps is also downfield–upfield–downfield. But now the order of the purine–purine clash steps is opposite, being minor groove–major groove–minor groove in 14-mer[4] while being major groove–minor groove–major groove in the pseudooperator. Because of the difference in alternating nucleotide sequence, the equivalent variation of ^{31}P shift simply suggests that the central regions of each sequence exist in different conformations.

14-mer[4] and 14-mer[5] are related by an "opposite" nucleotide sequence (a pyrimidine is replaced by the other pyrimidine and a purine is replaced by the other purine). This retains the purine–pyridimine base steps (and clashes) but obviously completely alters the sequence at every position. The ^{31}P chemical shift patterns of 14-mer[4] and 14-mer[5] are shown in Figure 7. Remarkably, the pattern of variation of ^{31}P chemical shifts and to a lesser extent ϵ/ζ of the two sequences is quite similar. The actual ^{31}P shifts and torsional angles between any two identical phosphate positions do differ slightly and can be attributed to base-sequence differences

affecting the local helical conformation.

Sequence-Specific Variations. Figure 5 compares the ^{31}P shift variation and the ϵ torsional angles to those of the predicted helical twist. The ^{31}P chemical shifts and ϵ (and ζ) torsional angles [directly derived from the experimentally measured J(P–H3′) coupling constants; see Experimental Procedures] follow essentially identical patterns (Figure 5). In those parts of the duplexes where the ^{31}P chemical shifts follow the Calladine rules (particularly at the ends of the duplex), we observe that the ϵ torsional angles also follow the predicted helix twist. In those base-pair steps where the ^{31}P chemical shifts do not fit the predicted Calladine rules (especially in the middle regions of the duplexes), we find that the ϵ torsional angles also do not follow the predicted helix twist values. This strongly supports our argument that ^{31}P chemical shifts are strongly dependent upon the backbone conformation. Furthermore these data suggest as we had previously concluded from our ^{31}P chemical shift studies (Gorenstein et al., 1988) that the backbone conformation does not appear to always follow the Calladine rules. As described in our previous paper (Gorenstein et al., 1988), ^{31}P shifts (and now also backbone torsional angles) follow the predicted helical adjustments from Calladine rules predominantly at the terminal sequences. However, the correlation is not strong, and the plot of ^{31}P chemical shift at all phosphate positions vs the predicted helical twist gives a correlation coefficient of only 0.60 (plot not shown; it is only slightly better if only the eight positions at the ends of the sequence are considered).

Correlation of J(P–H3′) Coupling Constants and ^{31}P Chemical Shifts. In our earlier work (Gorenstein et al., 1988) we had suggested that the sequence-specific variations in ^{31}P chemical shifts could be interpreted in terms of different conformational mixes of the B_I and B_{II} states. (The B_I conformational state is defined by $\zeta = g^-$, $\alpha = g^-$, $\epsilon = t$ and B_{II} by $\zeta = t$, $\alpha = g^-$, $\epsilon = g^-$; Dickerson, 1985.) As can be seen in Figures 5 and 8, there is a very good correlation between ^{31}P chemical shifts and J(P–H3′) coupling constants (correlation coefficient $R = 0.80$ at 18 °C). This correlation holds whether we compare only the nonclash positions ($R = 0.88$), Pu–Py clash positions ($R = 0.78$), Py–Pu clash positions ($R = 0.61$), or all clash positions ($R = 0.80$). Again, this strongly supports the hypothesis that the ^{31}P chemical shift variations are attributable to torsional angle changes. For example, the lowest downfield ^{31}P shift observed in a modest size oligonucleotide is around −3.8 ppm, whereas the most upfield ^{31}P shift is around −4.6 ppm. This then represents a range of ^{31}P chemical shift values of 0.8 ppm for all phosphate positions within an oligonucleotide sequence. If the ^{31}P chemical shift is determined solely by torsional angles ϵ and ζ, then the orientation of the phosphodiester backbone will take on conformations ranging in between fully g^-,t and t,g^- (B_{II} and B_I) states (referring to the ϵ,ζ torsional angles). Further analysis of the relationship between ^{31}P chemical shifts and measured torsional angles is described in Roongta et al. (to be submitted).

Limitations of Calladine Rules. Our analysis of the ^{31}P shifts and P–H3′ coupling constants of the pseudooperator and mutants confirms that some aspects of the Calladine rules are obeyed for variation of the sugar phosphate backbone of duplex oligonucleotide sequences in solution. Certainly the sum function rules have been experimentally verified in the crystal state due to the excellent correlations between the observed helical parameters and the corresponding sum function rules. Note, however, that the backbone torsional angles in the crystal state do not appear to follow any easily understandable rules

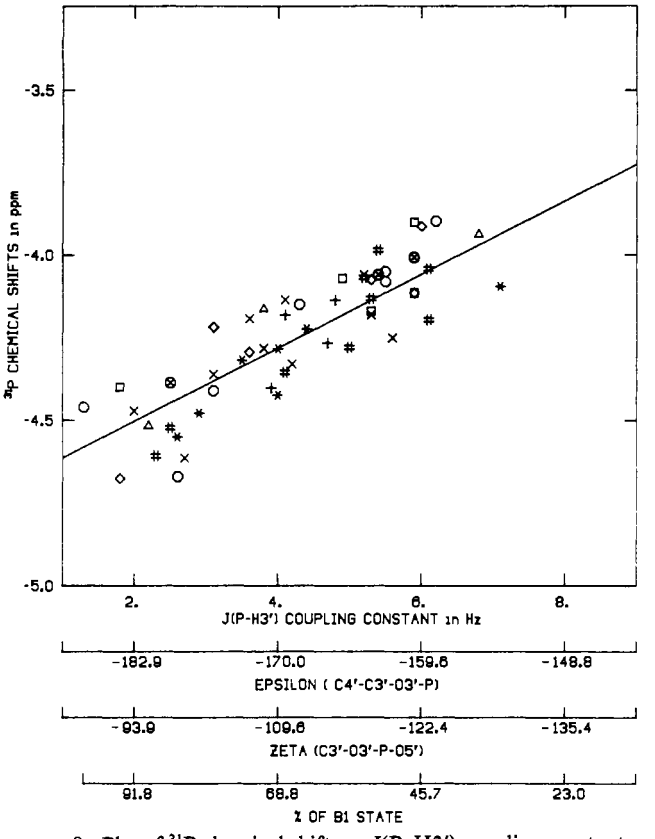

FIGURE 8: Plot of ^{31}P chemical shifts vs J(P–H3′) coupling constants, P–O3′ ester torsional angle ζ, C–O3′ torsional angle ϵ, and percent of the B_I state (Roongta et al., to be submitted) for the native 14-mer (◇), 14-mer[1] (+), 14-mer[3] (×), 14-mer[4] (#), and 14-mer[5] (*), at 18 °C. Additional symbols represent other 12-mer oligonucleotides (Roongta et al., to be submitted).

(Gorenstein et al., 1988). Furthermore, limitations of the Calladine rules in solution have been suggested from the solution structure of an asymmetrical 11-mer sequence (Clore & Gronenborn, 1985). Exactly opposite correlations were observed between certain helical parameters and those predicted by the sum function rules. In contrast, Feigon et al. (1983a,b) have observed helical parameters that correlated well with both predicted helical twist roll angle sum functions. Clearly the use of Calladine rules to predict various helical parameters is not universal for every oligonucleotide sequence, and some caution should therefore be taken in any type of interpretation with respect to Calladine sum function rules.

Conclusions and Some Suggestions Regarding DNA–Protein Recognition and Specificity Mediated through the Phosphate Ester Conformation. Most attention on DNA recognition has focused on primary base-pair specificity (Landschulz et al., 1988), defined as a direct readout mechanism (Matthews, 1988). As described in this paper, the conformation (as well as position) of the phosphates appears to show sequence specificity. It is thus not unrealistic to assume that at least a portion of protein–DNA recognition derives from recognition of the sequence-specific variation in the sugar phosphate backbone (an indirect readout mechanism). DNA is not a uniform cylinder of equivalently placed negative charges, but rather one in which the phosphate charges can significantly migrate across the surface of the cylinder in the response to changes in local helical parameters such as helix twist (in turn responsive to sequence specificity). With helical twist variations of 12–14° expected in normal B–DNA, the phosphate groups can vary from their uniform B–DNA position by ±7°, which translates into linear displacements of 1 Å. It would appear that the location of these

charges could represent a convenient signpost for designating a specific DNA sequence.

In phage 434 repressor (Anderson et al., 1987; Aggarwal et al., 1988), and λ repressor (Jordan & Pabo, 1988) the proteins make contacts to the base pairs as well as to the phosphates of the backbone. *Extensive* networks of hydrogen bonds are made with the oxygens of the phosphates in the direct operator recognition site. Certainly electrostatic interactions directly to the phosphates can be a major factor in stabilizing these complexes, but whether they represent a major part of the recognition code remains unanswered. Most significantly, in *trp* repressor it appears that most if not nearly all of the direct protein contacts to the operator are to the phosphate ester phosphoryl oxygens (Otwinowski et al., 1988). *No* direct hydrogen bonds exist between the base pairs of the operator and the repressor.

It is important to point out that changes in the torsional angles ϵ and ζ similar to the B_I to B_{II} conformational transitions not only shift the position of the phosphate but also rotate the orientation of the phosphoryl oxygens relative to the helix axis. As shown in the crystal structure of a 12-mer (Dickerson, 1983; Fratini et al., 1982), the plane formed by the phosphorus atom and the phosphoryl oxygens of the phosphate in the B_{II} conformation is nearly perpendicular to the plane formed by the phosphorus atom and the phosphoryl oxygens of the phosphates in the B_I conformation. Any set of H-bond donors or positively charged groups could readily discriminate between these two conformations that differ significantly in the orientation of their electrostatic potential. Our coupling constant and ^{31}P chemical shift data indicate that some phosphates have greater than 50% B_{II} conformational character. Certainly these structural differences are large enough that they could provide a signature of the base step. It is important to note that most of these direct protein–sugar phosphate contacts are mediated via amino acids with *short* polar side chains. Thus in λ repressor only Lys-26 in the loop containing Lys-24, Lys-25, and Lys-26 makes a possible contact with the operator phosphates. Obviously, if recognition is attributable to binding to the position *and* orientation of the phosphoryl oxygens, then long side chains cannot as effectively provide a unique readout of these phosphates. These sequence-specific variations in the conformation of the DNA sugar phosphate backbone thus can possibly explain the sequence-specific recognition of DNA by DNA binding proteins, as mediated through direct contacts and electrostatic complementarity between the phosphates and the protein. Perhaps a portion of the second genetic code will be found in the sequence-specific variation in the phosphate ester backbone, an often overlooked component of DNA structure.

ACKNOWLEDGMENTS

We greatly appreciate the contributions of Dr. Robert Santini and James Metz.

SUPPLEMENTARY MATERIAL AVAILABLE

Figure 3B–D showing 2D ^{31}P–^{1}H PAC heteronuclear correlation NMR spectra of 14-mers[2]–[4] and Figure 4B showing 2D ^{31}P–^{1}H *J*-resolved spectra of 14-mer[1] (5 pages). Ordering information is given on any current masthead page.

REFERENCES

Aggarwal, A. K., Rodgers, D. W., Drottar, M., Ptashne, M., & Harrison, S. C. (1988) *Science 242*, 899–907.

Anderson, J. E., Plashne, M., & Harrison, S. C. (1987) *Nature 326*, 846–852.

Arnott, S., Chandrasekaran, R., Hall, I. H., Puigjaner, L. C., Walker, J. K., & Wang, M. (1983) *Cold Spring Harbor Symp. Quant. Biol. 47*, 53–65.

Bax, A., & Freeman, R. (1981) *J. Magn. Reson. 44*, 542.

Berg, O. G., Winter, R. B., & Von Hippel, P. H. (1982) *Trends Biochem. Sci. 7*, 52.

Broido, M. A., Zon, G., & James, T. L. (1984) *Biochem. Biophys. Res. Commun. 119*, 663–670.

Calladine, C. R. (1982) *J. Mol. Biol. 161*, 343–352.

Caruthers, M. H. (1980) *Acc. Chem. Res. 13*, 155–160.

Cheng, D. M., Kan, L.-S., Miller, P. S., Leutzinger, E. E., & Ts'o, P. O. P. (1982) *Biopolymers 21*, 697–701.

Clore, G. M., & Gronenborn, A. M. (1983) *EMBO J. 2*, 2109–2115.

Clore, G. M., & Gronenborn, A. M. (1985) *EMBO J. 4*, 829–835.

Clore, G. M., Gronenborn, A. M., Moss, D. S. & Tickle, I. J. (1985) *J. Mol. Biol. 185*, 219–226.

Connolly, B. A., & Eckstein, F. (1984) *Biochemistry 23*, 5523–5527.

Dickerson, R. E. (1983) *J. Mol. Biol. 166*, 419–441.

Dickerson, R. E. (1985) *Biol. Macromol. Assem. 2*, 38–126.

Dickerson, R. E., & Drew, H. R. (1981) *J. Mol. Biol. 149*, 761–786.

Fegion, J., Leupin, W., Denny, W. A., & Kearns, D. R. (1983a) *Biochemistry 22*, 5943–5951.

Feigon, J., Leupin, W., Denny, W. A., & Kearns, D. R. (1983b) *Biochemistry 22*, 5930–5942.

Fratini, A. V., Kopka, M. L., Drew, H. R., & Dickerson, R. E. (1982) *J. Biol. Chem. 257*, 14686–14707.

Frechet, D., Cheng, D. M., Kan, L.-S., & Ts'o, P. O. P. (1983) *Biochemistry 22*, 5194–5200.

Fu, J. M., Schroeder, S. A., Jones, C. R., Santini, R., & Gorenstein, D. G. (1988) *J. Magn. Reson. 77*, 577–582.

Gait, M. J. (1984) *Oligonucleotide Synthesis: a Practical Approach*, IRL Press, Oxford.

Gorenstein, D. G. (1981) *Annu. Rev. Biophys. Bioeng. 10*, 355–386.

Gorenstein, D. G. (1983) *Prog. NMR Spectrosc. 16*, 1–98.

Gorenstein, D. G. (1984) *Phosphorus-31 NMR. Principles and Applications*, Academic, New York.

Gorenstein, D. G. (1987) *Chem. Rev. 87*, 1047–1077.

Gorenstein, D. G., & Findlay, J. B. (1976) *Biochem. Biophys. Res. Commun. 72*, 640.

Gorenstein, D. G., Findlay, J. B., Momii, R. K., Luxon, B. A., & Kar, D. (1976) *Biochemistry 15*, 3796–3803.

Gorenstein, D. G., Schroeder, S. A., Fu, J. M., Metz, J. T., Roongta, V. A., & Jones, C. R. (1988) *Biochemistry 27*, 7223–7237.

Gorenstein, D. G., Jones, C.R., Schroeder, S. A., Metz, J. T., Fu, J. M., Roongta, V. A., Powers, R., Karslake, C., Nikonowitz, E., & Santini, R. (1989) *NMR and Macromolecular Structure* (Niccolai, N., Ed.) Birkhauser, Boston (in press).

Groeddel, D. V., Yanasura, D. G., & Caruthers, M. H. (1978) *Proc. Natl. Acad. Sci. U.S.A. 75*, 3578–3582.

Hare, D. R., Wemmer, D. E., Chou, S. H., Drobny, G., & Reid, B. (1983) *J. Mol. Biol. 171*, 319.

James, T. L. (1984) *Phosphorus-31 NMR: Principles and Applications* (Gorenstein, D., Ed.) pp 349–400, Academic, Orlando, Fl.

Jones, C. R., Schroeder, S. A., & Gorenstein, D. G. (1988) *J. Magn. Reson. 80*, 370–374.

Jordan, S. R., & Pabo, C. O. (1988) *Science 242*, 893–899.

Kearns, D. R. (1984) *CRC Crit. Rev. Biochem. 15*, 237–290.

Kessler, H., Griesinger, C., Zarbock, J., & Loosli, H. R. (1984) *J. Magn. Reson. 57*, 331-336.
Lai, K., Shah, D. O., Derose, E., & Gorenstein, D. G. (1984) *Biochem. Biophys. Res. Commun. 121*, 1021.
Landschulz, W. H., Johnson, P. F., & McKnight, S. L. (1988) *Science 240*, 1759-1764.
Lankhorst, P. P., Haasnoot, C. A. G., Erkelens, C., & Altona, C. (1984) *J. Biomol. Struct. Dyn. 1*, 1387-1405.
Matthews, B. W. (1988) *Nature 335*, 294-295.
Miller, J. H., & Reznikoff, W. S. (1978) *The Operon*, Cold Spring Harbor Laboratory, Cold Spring Harbor, NY.
Ott, J., & Eckstein, F. (1985a) *Biochemistry 24*, 2530-2535.
Ott, J., & Eckstein, F. (1985b) *Nucleic Acids Res. 13*, 6317-6330.
Otwinowski, Z., Schevitz, R. W., Zhang, R. G., Lawson, C. L., Joachimiak, A., Marmorstein, R. Q., Luisi, B. F., & Sigler, P. B. (1988) *Nature 335*, 321.
Pardi, A., Walker, R., Rapoport, H., Wider, G., & Wüthrich, K. (1983) *J. Am. Chem. Soc. 105*, 1652.
Patel, D. J., Shapiro, L., & Hare, D. (1987) *Q. Rev. Biophys. 20*, 35-112.
Petersheim, M., Mehdi, S., & Gerlt, J. A. (1984) *J. Am. Chem. Soc. 106*, 439-440.
Reid, B. R. (1987) *Q. Rev. Biophys. 20*, 1-34.
Ribas-Prado, F., Giessner-Prettre, C., Pullman, B., & Daudey, J.-P. (1979) *J. Am. Chem. Soc. 101*, 1737.
Saenger, W. (1984) *Principles of Nucleic Acid Structure*, Springer-Verlag, New York.
Scheek, R. M., Boelens, R., Russo, N., Van Boom, J. H., & Kaptein, R. (1984) *Biochemistry 23*, 1371-1376.
Schroeder, S., Jones, C., Fu, J., & Gorenstein, D. G. (1986) *Bull. Magn. Reson. 8*, 137-146.
Schroeder, S. A., Fu, J. M., Jones, C. R., & Gorenstein, D. G. (1987) *Biochemistry 26*, 3812-3821.
Shah, D. O., Lai, K., & Gorenstein, D. G. (1984a) *Biochemistry 23*, 6717-6723.
Shah, D. O., Lai, K., & Gorenstein, D. G. (1984b) *J. Am. Chem. Soc. 106*, 4302.
Simons, A., Tils, D., von Wilcken-Bergmann, B., & Muller-Hill, B. (1984) *Proc. Natl. Acad. Sci. U.S.A. 81*, 1624-1628.
Sklenâř, V., & Bax, A. (1987) *J. Am. Chem. Soc. 109*, 7525-7526.
Sklenâř, V., Miyashiro, H., Zon, G., Miles, H. T., & Bax, A. (1986) *FEBS Lett. 208*, 94-98.
Takeda, Y., Ohlendorf, D. H., Anderson, W. F., & Matthews, B. W. (1983) *Science 221*, 1020-1026.
Van De Ven, F. J. M., & Hilbers, C. W. (1988) *Eur. J. Biochem. 178*, 1-38.

Transfer of Phospholipid and Protein into the Envelope of Gram-Negative Bacteria by Liposome Fusion†

Stephen Tomlinson,‡ Peter W. Taylor,§ and J. Paul Luzio*,‡

Department of Clinical Biochemistry, University of Cambridge, Addenbrooke's Hospital, Hills Road, Cambridge CB2 2QR, U.K., and Advanced Drug Delivery Research, Ciba-Geigy Pharmaceuticals, Wimblehurst Road, Horsham, West Sussex RH12 4AB, U.K.

Received February 21, 1989; Revised Manuscript Received June 14, 1989

ABSTRACT: A liposome–bacterial fusion system was developed in order to introduce preformed terminal complement complexes, C5b–9, into the outer membrane of Gram-negative bacteria. Liposomes were prepared from a total phospholipid extract of *Salmonella minnesota* Re595. Fusion between liposomes and *Salmonella* sp. or *Escherichia coli* 17 was dependent on time, temperature, pH, and Ca^{2+} and PO_4^- concentration. Only *Salmonella* sp. with attenuated LPS core regions were able to fuse efficiently with liposomes. It was demonstrated that fusion of liposomes with *S. minnesota* Re595 or *E. coli* 17 under optimum conditions resulted in (i) quantitative transfer of the self-quenching fluorescent membrane probe octadecyl rhodamine B chloride from the liposomal bilayer to the bacterial envelope, (ii) transfer of radiolabeled liposomal phospholipid to the bacterial outer membrane and its subsequent translocation to the cytoplasmic membrane, demonstrated by isolation of the bacterial membranes following fusion, and (iii) delivery of liposome–entrapped horseradish peroxidase (HRP) to the periplasmic space, confirmed by a chemiluminescent assay. Following fusion of liposomes incorporating C5b–9 complexes with *S. minnesota* Re595 or *E. coli* 17, immunological analysis of the isolated membranes revealed C5b–9 complexes located exclusively in the outer membrane.

Liposomes have been used extensively as model systems for the study of membrane interactions and membrane fusion. Fusion is an important event in many processes associated with eukaryotic cell activity and has been extensively investigated in relation to intracellular membrane traffic including endocytosis, exocytosis, and viral genomic delivery to host cells (White et al., 1983; Pastan & Willingham, 1985; De Lisle & Williams, 1986; Morre et al., 1988). In contrast, there is no intracellular vesicle transport system in prokaryotes, and it is at present unclear whether protein-controlled fusion events have any role to play in secretion, conjugation, and cell division in bacteria (Bamford et al., 1987).

† S.T. is supported by on SERC CASE postgraduate studentship.
‡ University of Cambridge.
§ Ciba-Geigy Pharmaceuticals.

0006-2960/89/0428-8303$01.50/0 © 1989 American Chemical Society